Oral Reference: ICF100897

EXTENSION OF THE UNIFIED APPROACH TO FATIGUE CRACK GROWTH TO ENVIRONMENTAL INTERACTIONS

K. Sadananda[1], R. L. Holtz[1] and A. K. Vasudevan[2]

[1] Code 6323, Materials Science and Technology Division,
Naval Research Laboratory, Washington D.C. 20375
[2] Office of Naval Research, Washington D.C. 22217

ABSTRACT

According to the Unified Approach for Fatigue Crack Growth developed by the authors. K_{max} and ΔK are two intrinsic parameters simultaneously required for quantifying fatigue crack growth data. The two parameters lead to two intrinsic thresholds that must be simultaneously exceeded for a fatigue crack to grow. Environmental interactions being time and stress-dependent processes affect fatigue crack growth through K_{max} parameter. Based on an extensive analysis of literature data, we have classified environmental effects into four basic types. The Unified Approach provides also a true reference state to define an inert fatigue behavior based on which one can quantify the environmental effects.

KEYWORDS

Fatigue crack growth, Environmental effects, Unified Approach, Classification of environmental effects

INTRODUCTION

In our Unified Approach to Fatigue [1-5], ΔK and K_{max} provide two crack tip driving forces simultaneously required for crack growth to occur. There are two corresponding thresholds that must be exceeded for a crack to grow. Crack growth data in terms of a ΔK vs K_{max} curve, show an L-shaped curve with two limiting values corresponding to two thresholds. At any other crack growth rates, the L-shaped curve shifts with the asymptotic limiting values, ΔK^* and $K_{max}{}^*$ increasing with crack growth rate, as shown in Fig. 1a.

CRACK GROWTH TRAJECTORY

In the Paris regime, when crack growth is governed typically by striation mechanisms, R-ratio

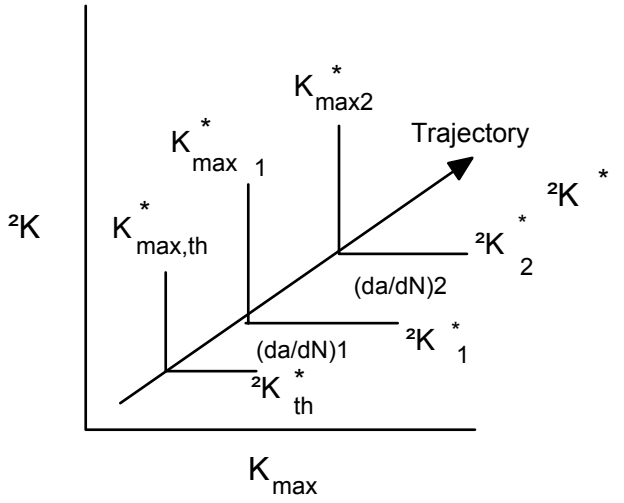

Fig. 1a. L-shaped curves defining ²K-Kmax limiting values at each crack growth rate

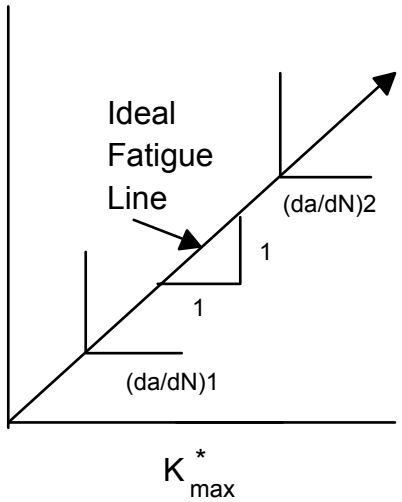

Fig. 1b. Trajectory of L-Shaped curves for an ideal fatigue case with no enviornmental effect

effects are minimal. Crack growth in this case is controlled purely by cyclic amplitude and

ΔK^* is nearly equal to K_{max}^*. Hence a plot of ΔK^* and K_{max}^* for different crack growth rates will be a straight line with $\Delta K^* = K_{max}^*$, as shown in Fig. 1b. The curve in Fig. 1b can be considered as a trajectory corresponding to crack growth mechanisms; the $\Delta K^* = K_{max}^*$ path characteristic of the pure-cycle controlled fatigue crack growth phenomenon. We refer to this as *ideal* fatigue behavior to separate it from other processes to be described below. Deviation from this line occurs if the crack growth mechanism changes. Empirically all deviations from ideal fatigue behavior occur with K_{max}^* being larger than ΔK^*, that is, all non-ideal behaviors fall below the line $\Delta K^* = K_{max}^*$. As the mechanisms become increasingly K_{max} controlled, the behavior swings more and more towards the K_{max}-axis.

CLASSIFICATION OF ENVIRONMENTAL EFFECTS

We have examined the available data in the literature for many different materials and environments, and arrived at some basic general classifications of the types of environmental interactions that are encountered during fatigue crack growth. We use the ΔK^*-K_{max}^* plot as a basis for the classification scheme. The plot represents the trajectory of crack growth behavior starting from threshold to unstable fracture as crack growth occurs, as suggested in Fig. 1a. For a given crack growth rate, the two values, ΔK^* and K_{max}^* represent the two limiting values in terms of the two parameters, ΔK and K_{max}, required for fatigue crack growth as defined in Fig. 1. The $\Delta K^* = K_{max}^*$ line represents the pure or ideal fatigue crack growth, Fig. 1b. This forms a reference line for the ideal inert behavior, which becomes a basis to classify the environmental contributions. This ideal behavior manifests only if the vacuum is very high or impurities in the so-called inert environments are very low and/or the materials are non-reactive to a given environment.

Fig 2 shows four types of basic behavior that are encountered. Type I behavior is typical of the true corrosion fatigue, wherein the environmental effects are maximum at low crack growth rates near threshold and decreases with increasing crack growth rate. At high crack growth rates, the reaction time is too short to have any significant environmental effect, and hence the behavior merges with that of ideal $\Delta K^*=K_{max}^*$ line. In a gas-metal system, four

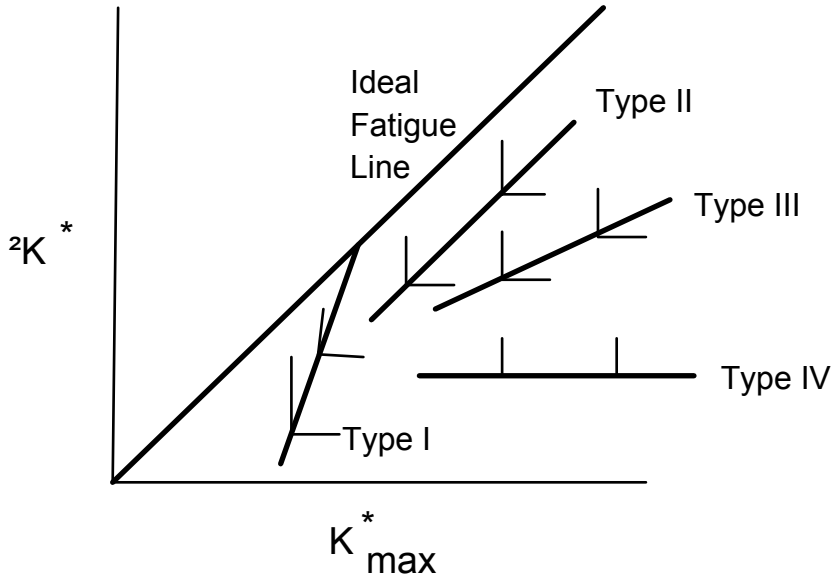

Fig. 2 Classification of Environmental Effects
Using Two-parameter aproach

sequential steps are considered[6]; transportation of aggressive species to the crack tip, reaction at the crack tip, transportation of the resulting hydrogen into the metal and finally the embrittlement of metal. In either case, with increasing crack growth rate, the Type I behavior is expected due to decreasing reaction time at the crack tip. Such a Type I behavior has indeed been observed.

The Type II behavior is indicated by the ΔK^*-K_{max}^* line parallel to the ideal behavior without merging with it. In this case, the environmental effects remain constant independent of crack growth rate or applied driving force, say K_{max}. Type II behavior is characterized by environmental effect that saturates extremely rapidly in relation to the transient crack advance times, and hence provides a constant contribution.

Type III behavior is opposite to Type I, wherein with increasing crack growth rate or K_{max}, the environmental contribution increases. Correspondingly the ΔK^*-K_{max}^* line swings towards K_{max}-axis. Here, transient time is not controlling, since with increasing crack growth rate or reduced time, the environmental contribution to fatigue crack growth actually increases rather than decreases. Since the deviation from ideal behavior of Type III increases with increasing stresses, it is associated with stress-enhanced or stress-driven environmental effects. Hence Type III may be more characteristic of stress corrosion fatigue process, Fig. 2b, in contrast to Type I and II. Increased effects of strain rates with increasing ΔK could also contribute to Type III.

Type IV is an extreme case of Type III behavior wherein the slope ΔK^*-K_{max}^* line approaches zero with ΔK^*-K_{max}^* trajectory running parallel to the K_{max}-axis, indicative of stress corrosion

crack growth rather than stress corrosion fatigue. The process is similar to static fatigue normally discussed with reference to ceramic materials. The role of cyclic stress in Type IV behavior may be to sharpen the crack tip, accentuating the stress-corrosion effect.

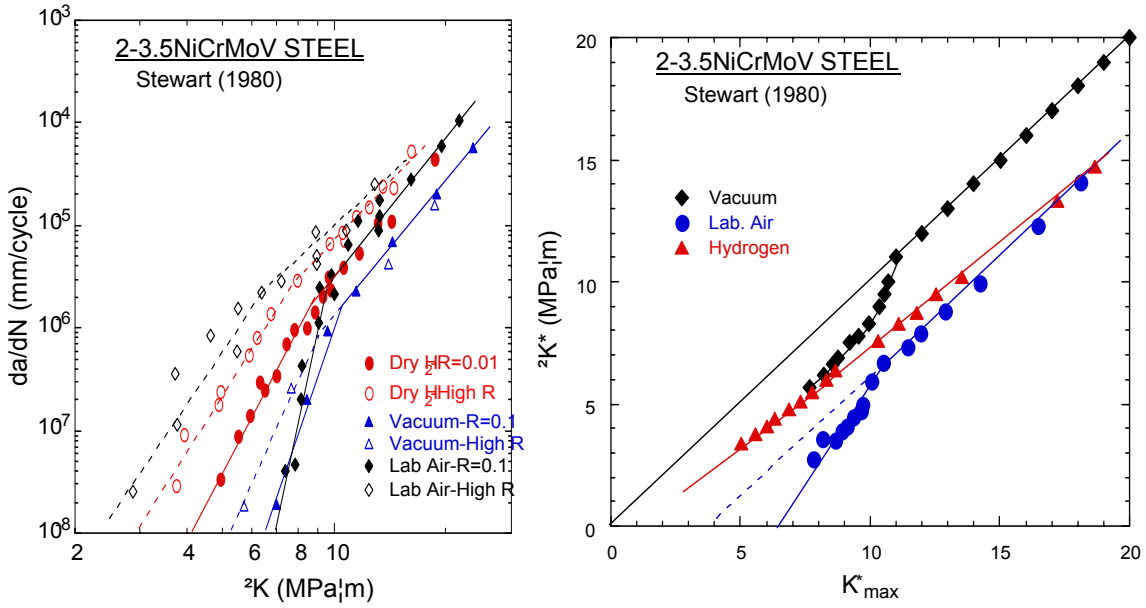

Fig. 3. A) Crack growth behavior in low alloy steel in ambient air, hydrogen and vacuum b) The analysis of the behavior in terms of ΔK*-Kmax* - trajectory map.

EXPERIMENTAL RESULTS

We show an example from the literature that illustrates a few of the types discussed above. To create the crack growth trajectory map similar to Fig. 2, both ΔK^* and K_{max}^* as a function of crack growth rate are needed. To determine these two values, crack growth rate data of a given material as a function of load ratio are needed. At the bare minimum, it is necessary to have data at R≈0 (e.g. R=0.05) from which we can estimate K_{max}^*, and the data at R ≈ 1 (e.g. R=0.9) from which we can estimate ΔK^*, since these are two asymptotic values at low and high R-values.

Fig. 3a shows the raw crack growth data in an ambient air, dry hydrogen and vacuum in low alloy steel (2-3.5Ni-Cr-Mo-V steel) measured by Stewart[7] at two R-ratios. The data may appear to be quite complex. However, since the data correspond to two extreme R-ratios, we can estimate the ΔK^* and K_{max}* values as a function of crack growth rate. These are plotted in the trajectory plot in Fig. 3b.

Considering first the data in vacuum, Fig. 3b shows that at low crack growth rates, the data deviate from the ideal fatigue behavior. But with increase in crack growth rates, the transient time decreases and the data slowly merge with that of the ideal fatigue behavior. The results demonstrate two important aspects. (a) The ideal fatigue behavior governed by the $\Delta K^*=K_{max}^*$ line can be observed in a material representing environment-free crack growth if the conditions are suitable. (b) The so-called vacuum tests do not ensure completely pure

inert environmental conditions since even very low partial pressures can have significant effect for some materials. This implies that care should be exercised in evaluating the environmental contributions using the vacuum tests as a reference. The vacuum data in Fig. 3b are consistent with the Type I behavior, that is decreasing environmental contribution with increasing crack growth rate until the data merge with the ideal fatigue behavior. The data are also consistent with Knudson flow[6] behavior where transportation of damaging species or the degree of crack-tip reaction reduces with the reduction in transient time due to increased da/dN and frequency or reduced partial pressure.

Examination of the laboratory air data of the same material shows somewhat different behavior from that of vacuum. It also shows initially a Type I behavior, but with increasing crack growth rate it converges to Type II behavior with data running parallel to the ideal line. Thus there is a definite change in the mechanism with increasing crack growth rate, stress or both. Here Type I leads to Type II behavior driven by applied stress, that is the mechanism in Type I should be such that it leads to a saturation stage at higher stresses or crack growth rates. One would expect that if the environmental effects are transportation control or reaction control then environmental contribution should decrease with increase in crack growth rate as in Type I. That is, one can have saturation effects at low crack growth rates due to larger reaction times available. From Fig. 2, saturation leading to unsaturation should result a Type II converging to Type I at high crack growth rates. One does not however expect an unsaturation leading to saturation that is a Type I behavior becoming Type II as the kinetics of the process are primarily time-dependent. On the other hand, if the process involves some complex roles of both time as well as stress, one can expect that it decreases due to decreasing time and stabilizing due to stress at some minimum value, causing a transition from Type I to Type II behavior. In order to establish the exact nature of the mechanism involved further analysis is required. Fig. 3, however, points out that controlling processes differ at ambient pressures from that observed in low vacuum.

The behavior in hydrogen environment differs from the previous two. At low crack growth rates the effect is comparable with that of partial vacuum and with increasing stress or growth rate the behavior converges to a constant effect similar to that of moist air. There is a small increase in environmental effect with crack growth typical of Type III, but that effect is very small. There is no Type I behavior observed at low crack growth rates in Hydrogen. Thus for the same material, three different environments show three different behaviors. Fig. 3 indicates that care should be exercised in interpretation of the data, particularly when there is change in the types of behavior in the same material and environment.

To understand the rate controlling process one has to examine in detail using above trajectory maps, the effect of frequency, composition and temperature (to evaluate the thermal activation process in each regime) supported by detailed fractographic analysis. Fig. 3, however, points to the fact one has to examine such trajectory map involving two crack tip driving forces, ΔK and K_{max}, to sort out the true contribution from environment in relation to the pure fatigue process. The micromechanism basis for each of the process has to be examined to have a better understanding of the mechanisms involved and how one mechanism can lead to the other with increasing crack growth rate. The analysis, however, points to the fact that environmental effects at the crack tip cannot be explained by a single mechanism for all crack growth rates, since they depend on both time and stress, as most of the corrosion process are. The reaction or transient time and the stress intensity at the crack tip have inverse relation

since the times are longer at low stresses and shorter at high stresses. Hence whether the process is dominated predominately by time or by stress will have significant effect on the resulting process and material response in the ΔK-Kmax* trajectory map. The Unified Approach points to the fact that ΔK-Kmax basis is fundamental for all fatigue crack growth process and the environmental effects have also to be examined from this perspective. Kmax parameter becomes a vehicle through which environmental effects get manifested, just as in the case of stress corrosion or sustained load crack growth processes. Analysis also provides a perspective in terms of the types of material behavior that one can expect, in addition to providing an environmentally pure fatigue behavior as a reference state.

SUMMARY AND CONCLUSIONS

We have extended the application of the Unified Approach to Fatigue Crack Growth to the analysis of environmental effects. It is shown that the two parameter approach is naturally amenable to the analysis since one of the governing driving force K_{max} is the characterizing parameter for the time-dependent environmental contributions. Based on this two-parameter approach we have developed a classification protocol for environmental contributions defining four types. This is discussed with reference to Fig. 3. Examples from the literature that exhibit the four types were shown.

REFERENCES

1. Vasudevan, A.K., Sadananda, K. and Louat, N., (1994), *Mater. Sci. Engrg*. 188, pp. 1-22.
2. Sadananda, K., and Vasudevan, A.K., (1993) in: *Fracture Mechanic,* Erodgan, R (Ed). ASTM-STP 1220, ASTM, 484-50.
3. Vasudevan, A.K. and Sadananda, K., (1995) *Met. Trans.A*, 26A, pp. 1221-34.
4. Sadananda, K. and Vasudevan, A.K., (1997) *Int. J. Fatigue*, 19, pp. S99-109.
5. Sadananda, K., Vasudevan, A.K., Holtz., R.L. and Lee, E.U., (1999) *Int. J. Fatigue*, 21, pp. S233-246.
6. Wei, R.P., and Simmons, G.W. (1981) *Int. J. Fracture*, 17, pp. 235-47
7. Stewart, A.T., (1980) *Engrg. Frac. Mech*., 13, pp. 463-78